13

All-Optical Wavelength-Selective Switch by Intensity Control in Cascaded Interferometers

Hiroki Kishikawa, Nobuo Goto and Kenta Kimiya
The University of Tokushima
Japan

1. Introduction

Wavelength-division-multiplexing (WDM) technology has been developing in broadband optical networks. The wavelength range used in fiber transmission systems has been increasing by employing various kinds of fiber amplifiers. In order to make it possible to handle signals of multiple wavelengths efficiently in network nodes, wavelength-selective processing in switching, routing and buffering systems will be required. In such processing systems, integrated-optic switches become one of fundamental key devices. In particular, high-speed wavelength-selective switches are required for WDM packet processing.

Wavelength-selective switches are classified from viewpoint of control method into electrically controlled devices and optically controlled ones. The former includes collinear acoustooptic (AO) devices (Goto & Miyazaki, 1990). Although multiple signals at different wavelengths can be independently switched with a single AO switch, it provides a response time only at an order of micro seconds. Optical circuits consisting of arrayed waveguide gratings (AWGs) and wavelength-insensitive switches are also regarded as a device in this class (Goh et al., 2008). The switching response depends on the control mechanizm of the wavelength-insensitive switches. The response time in thermo-optic switches is an order of milli seconds (Suzuki et al., 1998). On the other hand, optically controlled switches include devices using phase shift induced by optical nonlinear Kerr effect (Doran & Wood, 1988) and phase shift in semiconductor optical amplifiers (SOAs) (Nakamura et al., 2000) and in quantum dots (Kitagawa et al., 2009). These switches using phase shifting, in general, cannot provide wavelength-selectivity. Therefore, to realize wavelength-selective switching of the latter class, combination with multiplexers and demultiplexers such as AWGs is required.

As a switch of the latter class, the authors have proposed a new type of wavelength-selective switch where optical amplitudes in waveguide arms of interferometers are controlled by Raman amplifiers (Kishikawa & Goto, 2005; Kishikawa & Goto, 2006; Kishikawa & Goto, 2007a; Kishikawa & Goto, 2007b). In this article, the operation principle of wavelength-selective switching with the proposed devices is described. Computer simulation by finite-difference beam-propagation-method (FD-BPM) is performed to verify the switching operation.

2. Wavelength-selective switching by light control

Optical switching circuits discussed in this article consist of directional couplers, waveguide-type Raman amplifiers and attenuators as shown in Fig. 1. Designing of the

Source: Frontiers in Guided Wave Optics and Optoelectronics, Book edited by: Bishnu Pal,
ISBN 978-953-7619-82-4, pp. 674, February 2010, INTECH, Croatia, downloaded from SCIYO.COM

switching circuits indicated by the dotted rectangular is theoretically discussed in the next section. In the switching circuits, the signal light intensity is controlled with waveguide-type Raman amplifiers. We consider that WDM optical signals at wavelengths λ_1, λ_2 and λ_3 are incident into the upper waveguide of the circuit, and the two signals at λ_1 and λ_3 are to be switched to OUT B, whereas the signal at λ_2 is to be forwarded to OUT A. To induce this routing operation, optical pumping signals at λ_1' and λ_3' are injected to Raman amplifiers, where λ_i', i=1,2,3, is shorter than λ_i by an amount of a Raman shift λ_R, that is, $\lambda_i' = \lambda_i - \lambda_R$. The Raman shift depends on the material of the amplifier, whose typical value is approximately 100 nm. By injecting these pumping signals, the Raman amplifiers amplify wavelength-selectively the signals at λ_1 and λ_3. In some structures of the circuits, control signal λ_2' may be injected to another Raman amplifier placed in the circuits. We will find the structure of switching circuits with the required conditions for the amount of amplification. Since the Raman amplifiers are controlled by pumping light, all-optical switching can be realized.

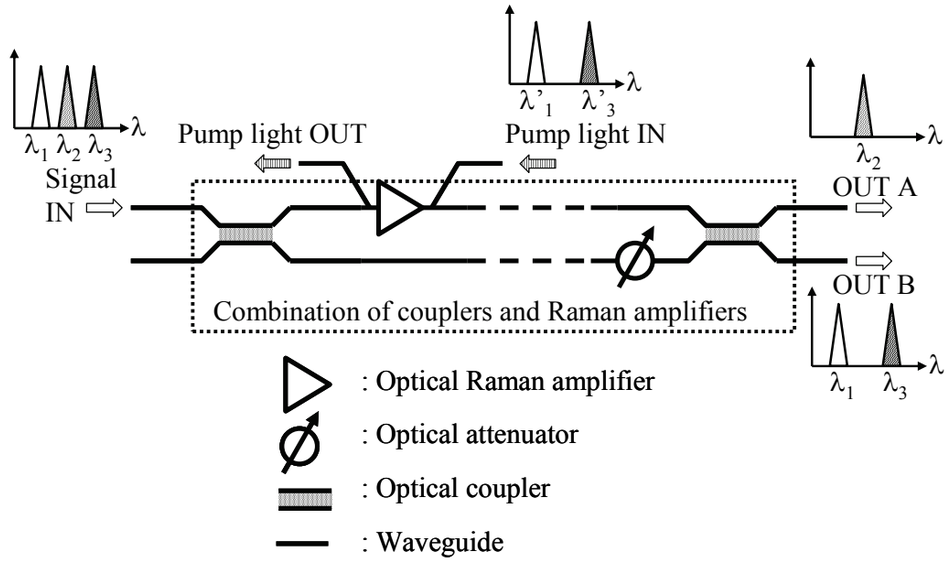

Fig. 1. Wavelength-selective switching circuit using a combination of optical couplers, optical Raman amplifiers and optical attenuators.

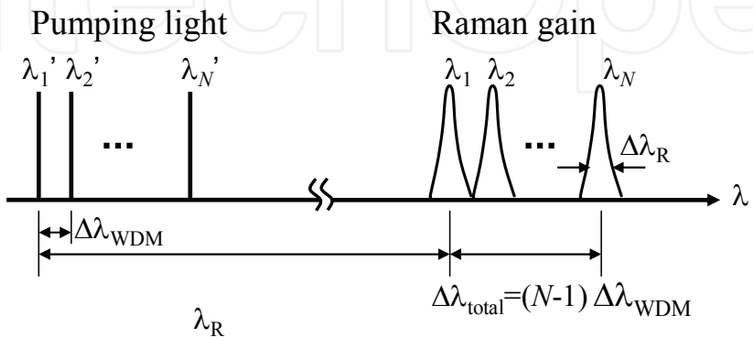

Fig. 2. Wavelength-selective amplification by stimulated Raman scattering with waveguide-type Raman amplifiers.

The wavelength-selective amplification can be performed in wide wavelength range by employing stimulated Raman scattering as shown in Fig. 2. The Raman gain bandwidth Δf_R in frequency for a specific pumping wavelength is tens GHz, for example, Δf_R =20 GHz with pulse-pumped maximum gain of 20 dB and continuous wave (cw)-pumped gain of 3.7 dB at λ =960 nm in GaP waveguides (Suto et al., 2002). In a Si waveguide, Δf_R =75 GHz with cw-pumped gain of 2.3 dB at wavelength 1574 nm (Rong et al., 2004), and pulse-pumped gain of 20 dB at wavelength 1673 nm (Raghunathan et al., 2005) were reported.

We denote the wavelength range available for this device as $\Delta\lambda_{total}$. Then, the WDM number handled with this switch is expressed as $N_{WDM} = \Delta\lambda_{total} / \Delta\lambda_R = c\,\Delta\lambda_{total} / \Delta f_R\,\lambda^2$, where c is the light velocity and $\Delta\lambda_R$ is the Raman gain bandwidth in wavelength. If $\Delta\lambda_{total}$ is as wide as 40 nm with the center wavelength of λ=1550 nm, N_{WDM} can be as large as 65 with Si Raman amplifiers.

2. Theoretical analysis of switching

2.1 Key elements

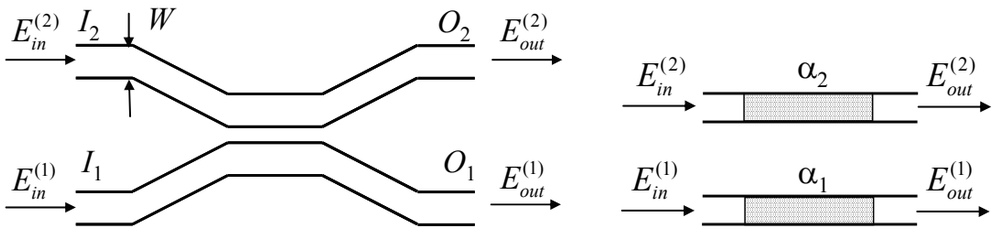

(a) directional coupler (b) parallel waveguides with amplifiers

Fig. 3. Key elements consisting the proposed wavelength-selective switches.

This section describes theoretical analysis with ideal device models. Key elements consisting the proposed switch are a 3-dB directional coupler and parallel independent waveguides containing amplifiers or attenuators as shown in Fig. 3. In the 3-dB directional coupler shown in (a), the electric field amplitude $E_{out}{}^{(i)}$, i=1, 2, of the optical output signals are related with $E_{in}{}^{(i)}$ of the optical input signals from the coupled mode theory, by eliminating the common phase term along the propagation, as

$$\begin{pmatrix} E_{out}^{(1)} \\ E_{out}^{(2)} \end{pmatrix} = \begin{pmatrix} \cos(\pi\kappa/4\kappa_0) & -j\sin(\pi\kappa/4\kappa_0) \\ -j\sin(\pi\kappa/4\kappa_0) & \cos(\pi\kappa/4\kappa_0) \end{pmatrix} \begin{pmatrix} E_{in}^{(1)} \\ E_{in}^{(2)} \end{pmatrix}, \tag{1}$$

where $j=\sqrt{-1}$, κ and κ_0 are the coupling coefficient and the coefficient at a designed wavelength for 3-dB coupling. The value κ depends on the field overlapping of optical individual waveguides. The wavelength dependence of κ therefore depends on the waveguide structure. This wavelength dependence of the 3-dB directional coupler causes the wavelength dependency in the proposed switch. At the designed wavelength for the 3-dB coupling, eq.(1) is simplified by using $\kappa = \kappa_0$, as

$$\begin{pmatrix} E_{out}^{(1)} \\ E_{out}^{(2)} \end{pmatrix} = \frac{1}{\sqrt{2}} \begin{pmatrix} 1 & -j \\ -j & 1 \end{pmatrix} \begin{pmatrix} E_{in}^{(1)} \\ E_{in}^{(2)} \end{pmatrix}. \tag{2}$$

Optical waves propagated along the independent parallel waveguides with amplification coefficient α_1 and α_2 are expressed as

$$\begin{pmatrix} E_{out}^{(1)} \\ E_{out}^{(2)} \end{pmatrix} = \begin{pmatrix} \alpha_1 & 0 \\ 0 & \alpha_2 \end{pmatrix} \begin{pmatrix} E_{in}^{(1)} \\ E_{in}^{(2)} \end{pmatrix}. \tag{3}$$

2.2 Switch A

We have proposed two switch architectures. Figure 4 shows the device structure of one of the switch architectures, named as switch A. The switch consists of two cascaded interferometers. In the first interferometer, each arm has a Raman amplifier with amplification coefficient α_A and α_B for the lower and upper arms, respectively. An attenuator with attenuation coefficient β is placed in the upper arm of the second interferometer. The Raman amplifiers are pumped by backward traveling light coupled with polarization-selective or wavelength-selective couplers.

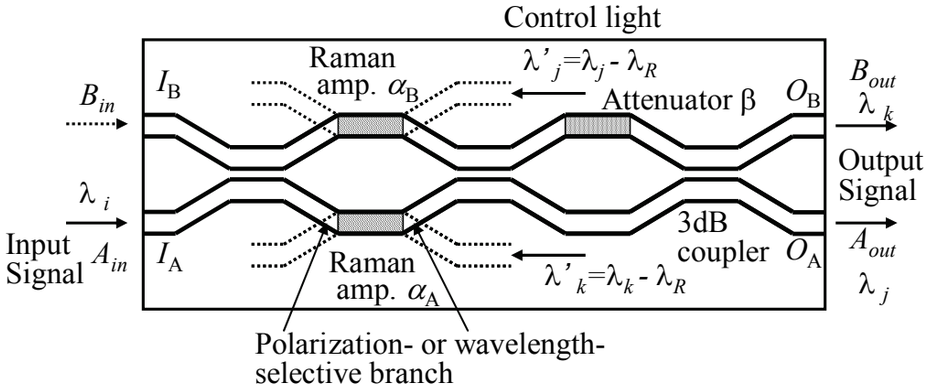

Fig. 4. Schematic diagram of the proposed wavelength-selective switch A consisting of two cascaded interferometers.

Optical WDM signals at wavelength λ_i, i=1, ..., N, are incident at input port I_A. When optical WDM signals at λ_k, $k \in \{1,...,N\}$, are to be switched to output port O_B, pumping WDM lights at λ_k' are coupled to the lower Raman amplifier to amplify the signals with gain coefficient α_A. The wavelength λ_k' satisfies the condition $\lambda_k' = \lambda_k - \lambda_R$. On the contrary, when the WDM signals at λ_j are to be switched to output port O_A, pumping WDM lights at λ_j' are coupled to the upper Raman amplifier to amplify the signals with gain coefficient α_B. Since the Raman amplifiers made of crystalline waveguides can wavelength-selectively amplify optical signals with narrow gain bandwidth $\Delta\lambda_R$, multiple WDM signals can be simultaneously and wavelength-selectively switched with this single switch.
Using eqs.(2) and (3), the output fields through the switch are related to the input fields as

$$\begin{pmatrix} A_{out} \\ B_{out} \end{pmatrix} = \left(\frac{1}{\sqrt{2}}\right)^3 \begin{pmatrix} 1 & -j \\ -j & 1 \end{pmatrix} \begin{pmatrix} 1 & 0 \\ 0 & \beta \end{pmatrix} \begin{pmatrix} 1 & -j \\ -j & 1 \end{pmatrix} \begin{pmatrix} \alpha_A & 0 \\ 0 & \alpha_B \end{pmatrix} \begin{pmatrix} 1 & -j \\ -j & 1 \end{pmatrix} \begin{pmatrix} A_{in} \\ B_{in} \end{pmatrix}. \tag{4}$$

Since the incident optical signal is coupled into the lower port I_A, we assume

$$\begin{pmatrix} A_{in} \\ B_{in} \end{pmatrix} = \begin{pmatrix} E_{in} \\ 0 \end{pmatrix}. \tag{5}$$

By substituting eq. (5) into eq. (4), the outputs are obtained as

$$\begin{pmatrix} A_{out} \\ B_{out} \end{pmatrix} = \frac{E_{in}}{2\sqrt{2}} \begin{pmatrix} \alpha_A - \alpha_B - \beta(\alpha_A + \alpha_B) \\ -j[\alpha_A - \alpha_B + \beta(\alpha_A + \alpha_B)] \end{pmatrix}. \tag{6}$$

It is expected from eq. (6) that B_{out}=0 for some values of α_A, α_B and β, on the other hand, A_{out}=0 for some other values of these parameters. Since the number of these unknown parameters is three for two equations, the solutions for these parameters cannot be determined. However, by considering physical limitations in these parameters, we obtain the solutions as

$$\begin{pmatrix} A_{out} \\ B_{out} \end{pmatrix} = \begin{cases} \begin{pmatrix} -E_{in} \\ 0 \end{pmatrix} & when \begin{cases} \alpha_A = 1 \\ \alpha_B = 1+\sqrt{2} \\ \beta = 1/(1+\sqrt{2}) \end{cases} \\ \begin{pmatrix} 0 \\ -E_{in} \end{pmatrix} & when \begin{cases} \alpha_A = 1+\sqrt{2} \\ \alpha_B = 1 \\ \beta = 1/(1+\sqrt{2}) \end{cases} \end{cases}. \tag{7}$$

It is found from eq.(7) that the switch operates as a 1x2 spatial switch whose output port is selected by proper amplification and attenuation effects. It is noted that the value β is constant in these two conditions. The incident light is routed to output port O_A by amplifying the upper amplifier with $\alpha_B = 1+\sqrt{2}$. The amplification is not required in the other amplifier α_A. On the contrary, the light is routed to output port O_B by amplifying the lower amplifier with $\alpha_A = 1+\sqrt{2}$. A drawback of this architecture is that either amplifier has to be activated for an input signal. That is, there is no default single output path without pumping.

2.3 Switch B

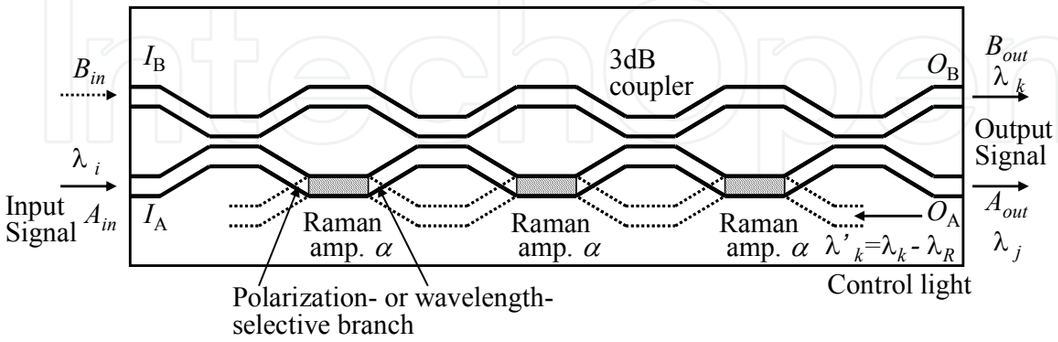

Fig. 5. Schematic diagram of the proposed wavelength-selective switch B consisting of three cascaded interferometers.

An alternative architecture of the switch consists of cascaded three interferometers as shown in Fig. 5. Three Raman amplifiers are placed in the lower arms of the three interferometers.

The feature of this architecture is that optical incident signals are routed to output port O_A without any pumping light for amplification, and are switched to output port O_B only when three amplifiers are activated by pumping. Since the three amplifiers are activated to have the same amplification coefficient α, the control for switching is simpler than that in switch A. The output fields through this switch are related to the input fields as

$$\begin{pmatrix} A_{out} \\ B_{out} \end{pmatrix} = \left(\frac{1}{\sqrt{2}}\right)^4 \begin{pmatrix} 1 & -j \\ -j & 1 \end{pmatrix} \begin{pmatrix} \alpha & 0 \\ 0 & 1 \end{pmatrix} \begin{pmatrix} 1 & -j \\ -j & 1 \end{pmatrix} \begin{pmatrix} \alpha & 0 \\ 0 & 1 \end{pmatrix} \begin{pmatrix} 1 & -j \\ -j & 1 \end{pmatrix} \cdot \begin{pmatrix} \alpha & 0 \\ 0 & 1 \end{pmatrix} \begin{pmatrix} 1 & -j \\ -j & 1 \end{pmatrix} \begin{pmatrix} A_{in} \\ B_{in} \end{pmatrix}. \tag{8}$$

Since the incident optical signal is coupled into the lower port I_A, we assume

$$\begin{pmatrix} A_{in} \\ B_{in} \end{pmatrix} = \begin{pmatrix} E_{in} \\ 0 \end{pmatrix}. \tag{9}$$

By substituting eq. (9) into eq. (8), the outputs are obtained as

$$\begin{pmatrix} A_{out} \\ B_{out} \end{pmatrix} = \frac{E_{in}}{4} \begin{pmatrix} \alpha^3 - 3\alpha^2 - \alpha - 1 \\ -j[\alpha^3 - \alpha^2 - \alpha + 1] \end{pmatrix}. \tag{10}$$

For no amplification at each Raman amplifier, that is α=1, output electric fields are calculated to be A_{out}= - E_{in} and B_{out}=0. It means that the incident optical wave is routed to output port O_A without amplification. In contrast, to switch the wave from output O_A to output O_B, the output electric fields have to be A_{out}=0 by proper amplification. The condition is given as a solution of an equation α^3-3α^2-α-1=0. This solution for α can be satisfied with α=3.383. With this value of α, B_{out} is calculated to be $-j(\alpha+1)(\alpha-1)^2 E_{in} = -j6.222\, E_{in}$. It means that the incident optical wave is amplified and routed to output O_B. This switching operation is summarized as

$$\begin{pmatrix} A_{out} \\ B_{out} \end{pmatrix} = \begin{cases} \begin{pmatrix} -E_{in} \\ 0 \end{pmatrix} & when \;\; \alpha = 1 \\ \begin{pmatrix} 0 \\ -j6.222E_{in} \end{pmatrix} & when \;\; \alpha = 3.383 \end{cases}. \tag{11}$$

The difference of the output intensity by a factor of $(6.222)^2$ can be compensated by employing an attenuator at output port O_B or an amplifier at output port O_A.

3. Numerical simulation of switching

3.1 Switch A

The switching characteristics can be analyzed using the equations described in the previous section. Wavelength dependence is also found by using eq. (1) instead of eq.(2) in the similar manner as described above. In this section, on the contrary, we verify the switching operation by numerical simulation to clarify the wave propagation along the waveguides of the switch. We use FD-BPM simulation with seventh-order Pade approximation (Hadley, 1992).

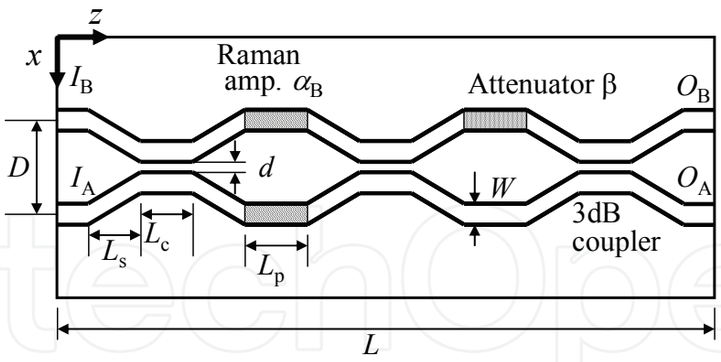

Fig. 6. Two-dimensional model of switch A for FD-BPM simulation.

We consider a two-dimensional slab waveguide model as shown in Fig. 6. The step length and the step width in the lateral direction are Δz=1.0 μm and Δx=0.05 μm, respectively. As the waveguide material, we consider silica waveguides. The core and cladding regions have refractive indices of n_c=1.461 and n_s=1.450, respectively. The width of the waveguide is W=3.0 μm. The interval and the length of the coupled region are set to be d=3.2 μm and L_c=100 μm to realize 3-dB coupling at wavelength 1550 nm. The length of the parallel waveguides corresponding to the Raman amplifiers and the attenuator is L_p=50 μm. The branching waveguides have the length of L_s=1025 μm. The distance between the two input ports is D=26.5 μm. The total length is L=6.65 mm.

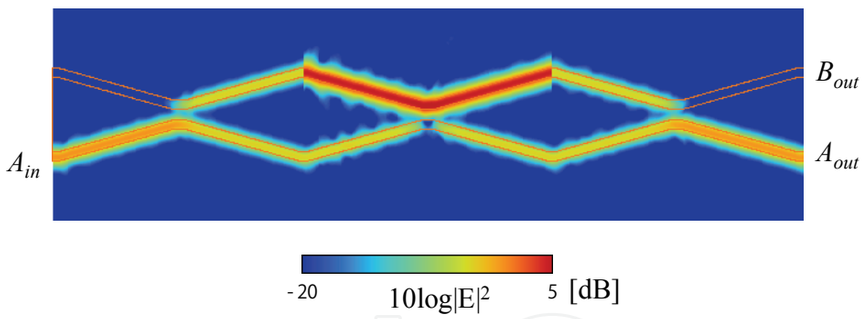

(a) $\alpha_A = 1,\ \alpha_B = 1+\sqrt{2},\ \beta = 1/(1+\sqrt{2})$

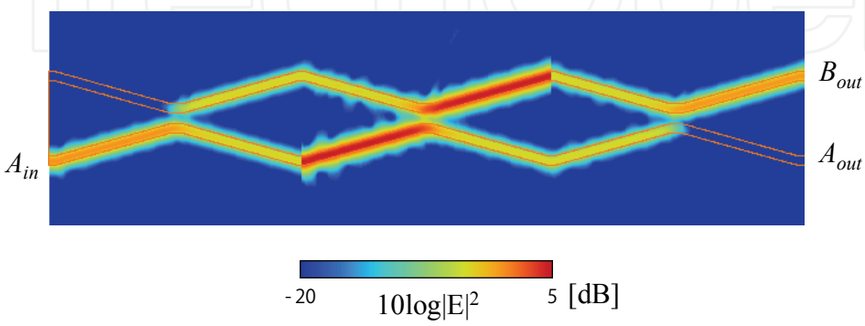

(b) $\alpha_A = 1+\sqrt{2},\ \alpha_B = 1,\ \beta = 1/(1+\sqrt{2})$

Fig. 7. Distribution of optical fields with two different switching conditions in swith A.

The switching operation at λ=1550 nm is confirmed as shown in Fig.7, where squared electric fields $|E|^2$ are plotted. In this simulation, Raman amplification is equivalently simulated just by increasing the optical electric field by multiplying the gain coefficient α_A or α_B at a place located at the end of the waveguide region for the amplifier. In a similar manner, the attenuator is modelled by multiplying the optical electric field by β at the beginning of the attenuator.

The wavelength dependence of the output intensity with the switch is plotted in Fig. 8. At the designed wavelength λ=1550 nm, the switching extinction ratio is larger than 35 dB. The wavelength range to achieve an extinction ratio larger than 20 dB is approximately 40 nm, though the 10-dB extinction ration is obtained over 100 nm. This wavelength dependence is caused by the wavelength dependence of the directional couplers.

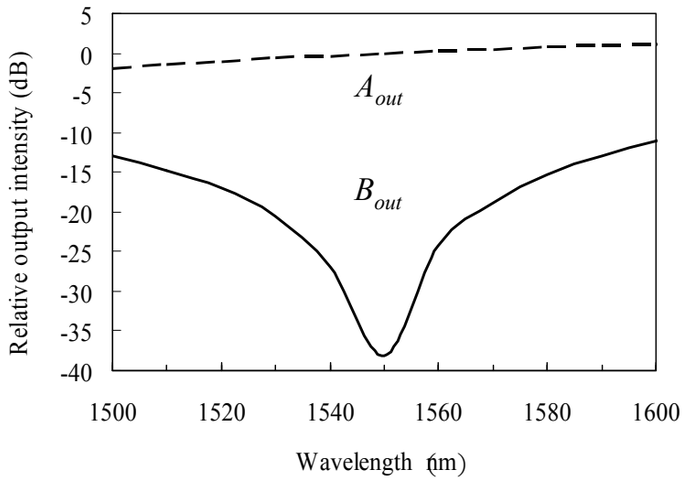

(a) $\alpha_A = 1,\ \alpha_B = 1+\sqrt{2},\ \beta = 1/(1+\sqrt{2})$

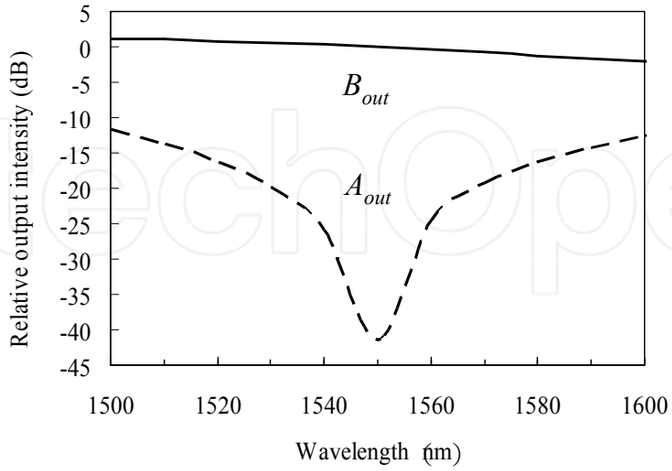

b) $\alpha_A = 1+\sqrt{2},\ \alpha_B = 1,\ \beta = 1/(1+\sqrt{2})$

Fig. 8. Wavelength dependence of switched outputs for the switch A designed at wavelength λ=1550nm.

3.2 Switch B

The switching operation with switch B is also verified by FD-BPM simulation. The model used in the simulation is shown in Fig. 9. The total length of the switch is L=8.85 mm.

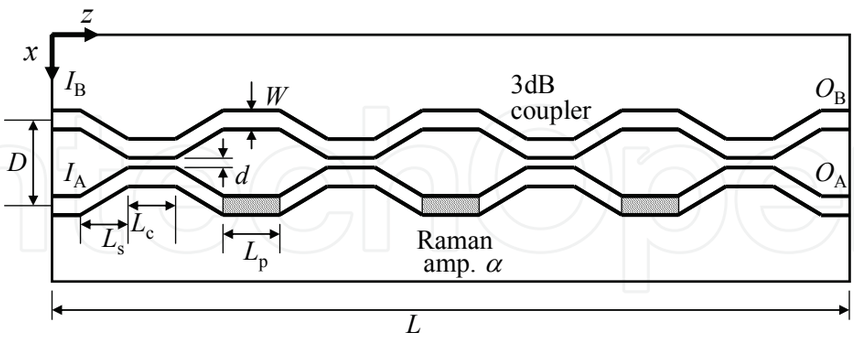

Fig. 9. Two-dimensional model of switch B for FD-BPM simulation.

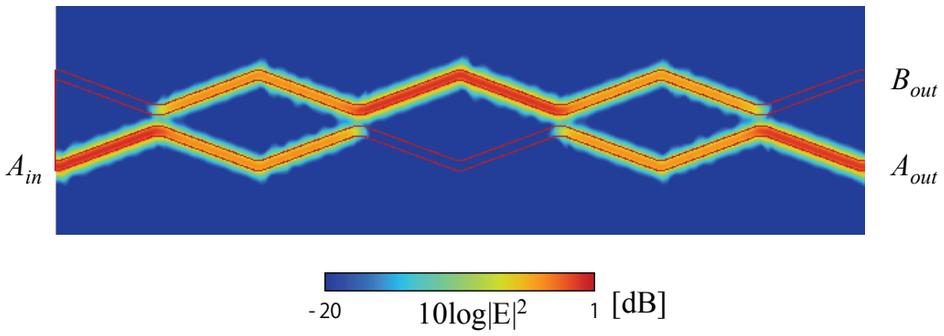

(a) $\alpha = 1$

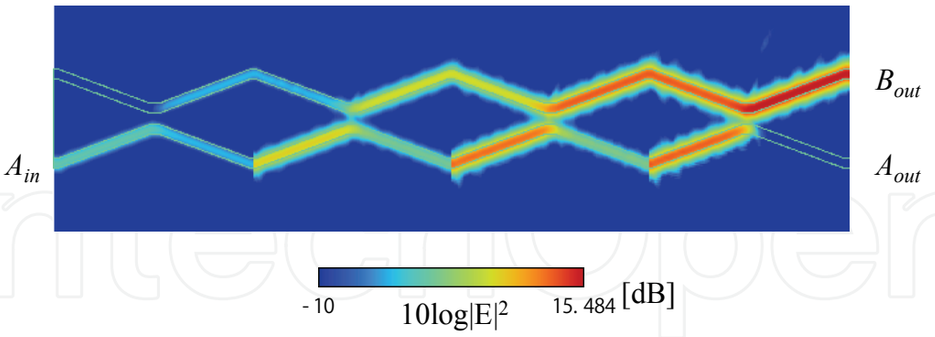

(b) $\alpha = 3.383$

Fig. 10. Distribution of optical fields with two different switching conditions in swith B.

The switching operation at λ=1550 nm is confirmed as shown in Fig. 10. Although the output intensities from output port O_A and O_B are different, switching is successfully simulated.
The wavelength dependence is shown in Fig. 11. At the designed wavelength λ=1550nm, the switching extinction ratio is larger than 25 dB. The wavelength range to achieve the extinction ratio larger than 20 dB is approximately 30 nm, though the 10-dB extinction ration is obtained over 80 nm.

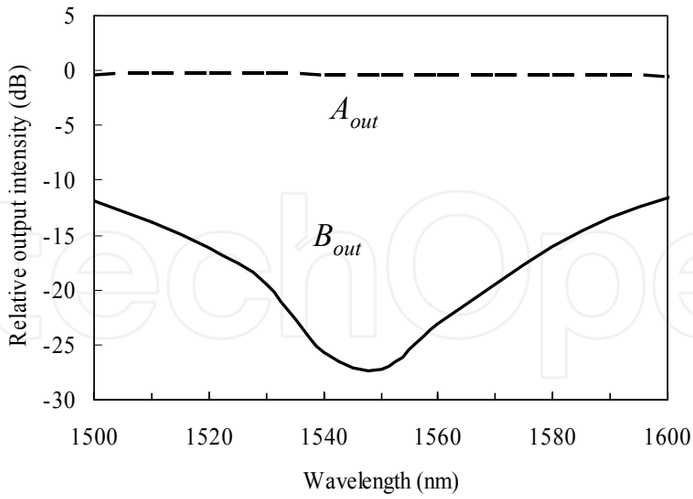

(a) $\alpha = 1$

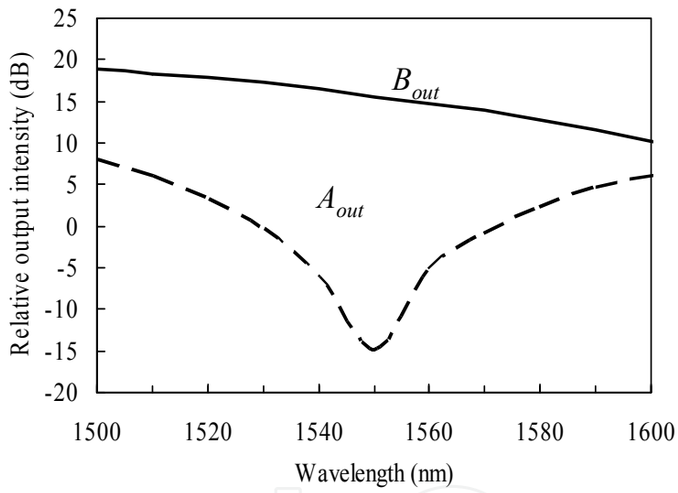

(b) $\alpha = 3.383$

Fig. 11. Wavelength dependence of switched outputs for the switch B designed at wavelength λ=1550nm.

4. Improvement of wavelength dependency

Waveguide-type Raman amplifiers do not depend on wavelength bands to be used because stimulated Raman scattering which is the base effect of Raman amplification can occur at any wavelength bands. Meanwhile, 3dB couplers have wavelength dependency in general, that is, the function of dividing an incident optical wave into two waves at the rate of 50:50 is available at some particular wavelength bands. The main cause of the wavelength dependency is the wavelength dependence of the coupling coefficient κ in eq.(1). For improving the characteristics of wavelength dependency of the switch and utilizing it at any

wavelength bands, wavelength-independent (or wavelength-flattened) optical couplers should be employed. Fiber-type wavelength-independent couplers, that can be used for 50:50 of the dividing rate at wavelength bands such as 1550 nm± 40 nm and 1310 nm ± 40 nm, have already been on the market. However, waveguide-type wavelength-independent couplers have advantage from the viewpoint of integrating the switch elements.
An alternative for improving wavelength dependence is to replace the directional couplers by asymmetric X-junction couplers (Izutsu et al., 1982; Burns & Milton, 1980; Hiura et al., 2007). The asymmetric X-junction coupler has basically no dependence on wavelength and helps to improve the wavelength dependency of the proposed switch (Kishikawa et al., 2009a; Kishikawa et al., 2009b).

5. Another issue in implementation

Phase shift of the signal pulse experienced in the waveguide-type Raman amplifiers should be discussed because it can impact the operation of the switch. The phase shift is induced from refractive index change caused by self-phase modulation (SPM), cross-phase modulation (XPM), free carriers generated from two-photon absorption (TPA) (Roy et al., 2009), and temperature change. Although the structure of the switch becomes more complex, the effect of SPM and TPA-induced free carriers can be cancelled by installing the same nonlinear waveguides as those of the waveguide-type Raman amplifiers into counter arms of the Mach-Zehnder interferometers of the switch. The influence of XPM and temperature change involved with high power pump injection can also be suppressed by injecting pump waves, having the same power and different wavelengths that do not amplify the signal pulse, into the counterpart nonlinear waveguides.

6. Conclusion

We proposed a novel all-optical wavelength-selective switching having potential of a few tens of picosecond or faster operating speed. We discussed the theory and the simulation results of the switching operation and the characteristics. Moreover, the dynamic range over 25dB was also obtained from the simulation results of the switch. This characteristics can be wavelength-selective switching operation. More detailed analysis and simulation taking the nonlinearity of Raman amplifiers into account are required to confirm the operation with actual devices.
Although the principle and the fundamental verification were performed with the switches consisting of directional couplers, the idea can be similarly applied to switches consisting of other components such as asymmetric X-junction couplers to increase the wavelength range.

8. References

Doran, N. J. & Wood, D. (1988). Nonlinear-Optic Loop Mirror, Optics Lett., vol.13, no.1, pp.56-58, Jan. 1988.

Burns, W. K. & Milton, A. F. (1980). An Analytic Solution for Mode Coupling in Optical Waveguide Branches, IEEE J. Quantum Electron., vol.QE-16, no.4, pp.446-454, Apr. 1980.

Goh, T., Kitoh, T., Kohtoku, M., Ishii, M., Mizuno, T. & Kaneko, A. (2008). Port Scalable PLC-Based Wavelength Selective Switch with Low Extinction Loss for Multi-Degree ROADM/WXC, The Optical Fiber Communication Conference and the National Fiber Optic Engineers Conference (OFC/NFOEC2008), San Diego, OWC6, Mar. 2008.

Goto, N & Miyazaki, Y. (1990). Integrated Optical Multi-/Demultiplexer Using Acoustooptic Effect for Multiwavelength Optical Communications, IEEE J. on Selected Areas in Commun., vol.8, no.6, pp.1160-1168, Aug. 1990.

Hadley, G. R. (1992). Wide-Angle Beam Propagation Using Pade Approximant Operators, Opt. Lett., vol.17, no.20, pp.1426-1428, Oct. 1992.

Hiura, H., Narita, J. & Goto, N. (2007). Optical Label Recognition Using Tree-Structure Self-Routing Circuits Consisting of Asymmetric X-junction, IEICE Trans. Commun., vol.E90-C, no.12, pp.2270-2277, Dec. 2007.

Izutsu, M., Enokihara, A. & Sueta, T. (1982). Optical-Waveguide Hybrid Coupler, Opt. Lett., vol.7, no.11, pp.549-551, Nov. 1982.

Kishikawa, H. & Goto, N. (2005). Proposal of All-Optical Wavelength-Selective Switching Using Waveguide-Type Raman Amplifiers and 3dB Couplers, J. Lightwave Technol., vol.23, no.4, pp.1631-1636, Apr. 2005.

Kishikawa, H. & Goto, N. (2006). Switching Characteristics of All-Optical Wavelength-Selective Switch Using Waveguide-Type Raman Amplifiers and 3-dB Couplers, IEICE Trans. Electron., vol.E89-C, no.7, pp.1108-1111, July 2006.

Kishikawa, H. & Goto, N. (2007a). Optical Switch by Light Intensity Control in Cascaded Coupled Waveguides, IEICE Trans. Electron., vol.E90-C, no.2, pp.492-498, Feb. 2007.

Kishikawa, H. & Goto, N. (2007b). Designing of Optical Switch Controlled by Light Intensity in Cascaded Optical Couplers, Optical Engineering, vol.46, no.4, pp.044602-1-10, Apr. 2007.

Kishikawa, H., Kimiya, K., Goto, N. & Yanagiya, S. (2009a). All-Optical Wavelength-Selective Switch Controlled by Raman Amplification for Wide Wavelength Range, Optoelectronics and Communications Conf., OECC2009, Hong Kong, TuG3, July 2009.

Kishikawa, H., Kimiya, K., Goto, N. & Yanagiya, S. (2009b). All-Optical Wavelength-Selective Switch by Amplitude Control with a Single Control Light for Wide Wavelength Range", Int. Conf. on Photonics in Switching, PS2009, Pisa, PT-12, Sept. 2009.

Kitagawa, Y., Ozaki, N., Takata, Y., Ikeda, N., Watanabe, Y., Sugimoto, Y. & Asakawa, K. (2009). Sequential Operations of Quantum Dot/Photonic Crystal All-Optical Switch With High Repetitive Frequency Pumping, J. Lightwave Technol., vol.27, no.10, pp.1241-1247, May 2009.

Nakamura, S., Ueno, Y., Tajima, K., Sasaki, J., Sugimoto, T., Kato, T., Shimoda, T., Itoh, M., Hatakeyama, H., Tamanuki, T. & Sasaki, T. (2000). Demultiplexing of 168-Gb/s Data Pulses with a Hybrid-Integrated Symmetric Mach-Zehnder All-Optical Switch, IEEE Photon. Tech. Lett., vol.12, no.4, pp.425-427, Apr. 2000.

Raghunathan, V., Boyraz, O & Jalali, B. (2005). 20dB On-Off Raman Amplifiation in Silicon Waveguides, Conf. Lasers and Electro-Optics (CLEO2005), Baltimore, CMU1, May 2005.

Rong, H., Liu, A., Nicolaescu, R., Paniccia, M., Cohen, O. & Hak, D. (2004). Raman Gain and Nonlinear Optical Absorption Measurements in a Low-Loss Silicon Waveguide, Appl. Phys. Lett., vol.85, no.12, pp.2196-2198, Sept. 2004.

Roy, S., Bhadra, S. K. & Agrawal, G. P. (2009). Raman Amplification of Optical Pulses in Silicon Waveguides: Effects of Finite Gain Bandwidth, Pulse Width, and Chirp, J. Opt. Soc. Am. B, vol. 26, no. 1, Jan. 2009.

Suto, K., Saito, T., Kimura, T., Nishizawa, J. & Tanabe, T. (2002). Semiconductor Raman Amplifier for Terahertz Bandwidth Optical Communication, J. Lightwave Technol., vol.20, no.4, pp.705-711, Apr. 2002.

Suzuki, S., Himeno, A. & Ishii, M. (1998). Integrated Multichannel Optical Wavelength Selective Switches Incorporating an Arrayed-Waveguide Grating Multiplexer and Thermooptic Switches, J. Lightwave Technol., vol.16, no.4, pp.650-655, Apr. 1998.

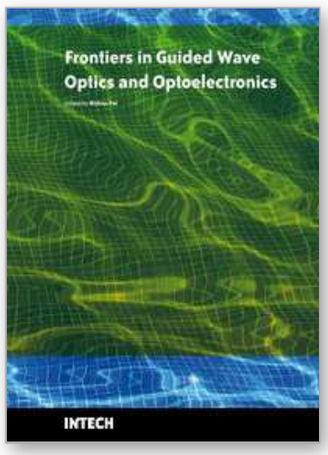

Frontiers in Guided Wave Optics and Optoelectronics
Edited by Bishnu Pal

ISBN 978-953-7619-82-4
Hard cover, 674 pages
Publisher InTech
Published online 01, February, 2010
Published in print edition February, 2010

As the editor, I feel extremely happy to present to the readers such a rich collection of chapters authored/co-authored by a large number of experts from around the world covering the broad field of guided wave optics and optoelectronics. Most of the chapters are state-of-the-art on respective topics or areas that are emerging. Several authors narrated technological challenges in a lucid manner, which was possible because of individual expertise of the authors in their own subject specialties. I have no doubt that this book will be useful to graduate students, teachers, researchers, and practicing engineers and technologists and that they would love to have it on their book shelves for ready reference at any time.

InTech Europe
University Campus STeP Ri
Slavka Krautzeka 83/A
51000 Rijeka, Croatia
Phone: +385 (51) 770 447
Fax: +385 (51) 686 166
www.intechopen.com

InTech China
Unit 405, Office Block, Hotel Equatorial Shanghai
No.65, Yan An Road (West), Shanghai, 200040, China
中国上海市延安西路65号上海国际贵都大饭店办公楼405单元
Phone: +86-21-62489820
Fax: +86-21-62489821

IntechOpen